Electronic Supplementary Material (ESI) for Dalton Transactions.

Supporting Information for

A novel copper-rich open-framework chalcogenide with chiral topology constructed from distinctive bimetallic [Cu_5SnSe_{10}] clusters

Yinan Kong,[a‡] Yayun Ding,[a‡] Chengdong Liu,[a] Jiaxu Zhang,[a] Rui Zhou,[a] Dong-Sheng Li,[c] Ning Chen,[a] Xiang Wang*[a] and Tao Wu*[b]

[a] College of Chemistry, Chemical Engineering and Materials Science, Soochow University, Suzhou, Jiangsu 215123, China

[b] College of Chemistry and Materials Science, Guangdong Provincial Key Laboratory of Functional Supramolecular Coordination Materials and Applications, Jinan University, Guangzhou, Guangdong 510632, China.

[c] College of Materials and Chemical Engineering, Hubei Provincial Collaborative Innovation Center for New Energy Microgrid, Key Laboratory of Inorganic Nonmetallic Crystalline and Energy Conversion Materials, China Three Gorges University, Yichang, Hubei 443002, China

* Corresponding author E-mails: *light@suda.edu.cn* and *wutao@jnu.edu.cn*

Experimental Section

Chemicals and Materials. Copper iodide (CuI, 99.99%), tin powder (Sn, 99.9%), selenium powder (Se, 99.9%), sulfur powder (S, ≥ 99.5%), deionized water (H_2O), 1,5-diazabicyclo[4.3.0]non-5-ene (DBN, ≥ 98%) were commercially available and used without further purification.

Synthesis of COC-10-Se. A mixture of copper iodide (42 mg, 0.22 mmol), tin powder (51 mg, 0.43 mmol), selenium powder (109 mg, 1.38 mmol), deionized water (H_2O, 0.5 mL), 1,5-diazabicyclo[4.3.0]non-5-ene (DBN, 1.5 mL) was stirred in a 23 mL Teflon-lined stainless steel autoclave for twenty minutes. After the vessel was sealed and heated at 170^{o}C for 8 days, the autoclave was taken out and gradually cooled to room temperature. A large number of red block crystals were obtained after three times of ethanol ultrasonic washing and filtration. The phase purity of the sample was identified by powder X-ray diffraction measurements.

Synthesis of COC-10-SeS. The mixture of copper iodide (42 mg, 0.22 mmol), tin powder (51 mg, 0.43 mmol), selenium powder (60 mg, 0.76 mmol), sulfur powder (30 mg, 0.94 mmol), deionized water (H_2O, 0.5 mL) and 1,5-diazabicyclo[4.3.0]non-5-ene (DBN, 1.5 mL) was placed in a 23 mL Teflon-lined stainless steel autoclave and stirred for 30 minutes, s After the vessel was sealed and heated at 170^{o}C for 8 days. The autoclave was then taken out and cooled to room temperature. A large number of red block crystals were obtained after three times of ethanol ultrasonic washing and filtration. The elemental analysis results are consistent with the above crystals.

Single-Crystal X-ray Diffraction Characterization. The single-crystal X-ray diffraction (SCXRD) measurements on **COC-10-Se** was performed on a Bruker Smart CPAD area diffractometer with nitrogen-flow temperature controller using graphite-monochromated Mo-Kα (λ= 0.71073 Å) radiation at 120 K. The structure was solved by direct method using SHELXS-2014 and the refinement against all reflections of the compound was performed using SHELXL-2014. All the protonated organic amine (DBN-H^+) and H_2O molecules indicated by the TGA, FT-IR and EA results were squeezed by the *PLATON* program for better quality of crystal data.

Powder X-ray Diffraction Characterization. The Powder X-ray Diffraction (PXRD) data were collected on a desktop diffractometer (D2 PHASER, Bruker, Germany) using Cu-Kα (λ=1.54056 A) radiation operated at 30 kV and 10 mA. The samples were ground into fine powders for several minutes before the test.

Elemental Analysis. Energy dispersive spectroscopy (EDS) analysis was performed on scanning electron microscope (SEM) equipped with EDS detector. An accelerating voltage of 25 kV and 40 s accumulation time were applied. Elemental analysis of C, H, and N was performed on VARIDEL III elemental analyzer. (**COC-10-Se**, *Calcd.*: C, 13.60; N, 4.53; H, 2.06 *wt*%. *Found:* C, 12.86; N, 4.13; H, 1.98 *wt*%; **COC-10-SeS**, *Calcd.*: C, 13.90 N, 4.64; H, 2.25 *wt*%. *Found:* C, 12.79; N, 4.18; H, 1.91 *wt*%).

Thermogravimetric Measurement. A Shimadzu TGA-50 thermal analyzer was used to measure the thermogravimetric (TG) curve by heating the sample from room temperature to 800 °C with heating rate of 10 °C/min under N_2 flow.

Fourier Transform Infrared Absorption. Fourier transform infrared (FT-IR) spectral analysis was performed on a Thermo Nicolet Avatar 6700 FT-IR spectrometer with diamond/zinc selenide optics allowing the instrument to observe from 600-4000 cm^{-1}.

UV-Vis diffusion reflectance spectra. Room-temperature solid-state UV-Vis diffusion reflectance spectra (UV-Vis DRS) of **COC-10-Se** and **COC-10-SeS** were measured on a SHIMADZU UV-3600 UV-Vis-NIR spectrophotometer coupled with an integrating sphere by using $BaSO_4$ powder as the reflectance reference. In order to determine the band edge of the direct-gap semiconductor, the relation between the absorption coefficients (α) and the incident photon energy (hv) is exhibited as $\alpha hv = A(hv\text{-}Eg)^{0.5}$, where A is a constant that relates to the effective masses associated with the valence and conduction bands, and Eg is the optical transition gap of the solid material. By extrapolating the linear region to the abscissa, the band gap can be estimated.

X-ray photoelectron spectroscopy. X-ray photoelectron spectroscopy (XPS) was collected with a Leeman prodigy spectrometer equipped with a monochromatic Al Kα X-ray source and a concentric hemispherical analyzer.

Preparation of COC-10-Se/ITO Film and COC-10-SeS/ITO Film. To prepare the working electrode, 2 mg of COC-10-Se/COC-10-SeS crystals were first ground into fine powders, and then added into 60 μL of 0.5% nafion (D-521 dispersion, 5% in water and 1-propanol). After ultrasonic treatment for 30 minutes, the obtained suspensions were dropped onto the surface of ITO substrate, and then dried at room temperature.

Transient photocurrent and electrochemical impedance spectroscopy measurement. The transient photocurrent and electrochemical impedance spectroscopy (EIS) experiments were carried out on a CHI760E electrochemistry workstation in a standard three-electrode configuration. The sample coated ITO glass electrode (effective area about 1 cm^2), the saturated calomel electrode (SCE), and the Pt plate electrode were used as the working electrode, reference electrode and auxiliary electrode, respectively. The light source was a 150 W high pressure xenon lamp with a horizontal of 25 cm away from the surface of the ITO working electrode. Sodium sulphate aqueous solution (0.5 M, 100 mL) was used as the supporting electrolyte.

Photocatalytic Degradation of MB. The photocatalytic reactions under full-spectra (200-800 nm) irradiation for the degradation of MB were performed in a glass bottle. A 300 W Xe lamp was used as illuminating source. Crystalline **COC-10-Se** and **COC-10-SeS** photocatalyst (8 mg) were added into 15 mL MB aqueous solution (1.20×10^{-5} M) and stirring for 45 min in the dark condition to reach the adsorption/desorption equilibrium, respectively. The resulting solution was analyzed by UV-1800 UV-vis spectrophotometer every 10 minutes. The degradation efficiency was calculated as C_t/C_0, where C_t and C_0 represent the main peak of absorption at each irradiated time interval and the concentration of MB after adsorption/desorption equilibrium, respectively.

Ion Exchange. The sample of COC-10-Se (10 mg) and COC-10-SeS (10 mg) were dipped in 10 mL aqueous solution of CsCl (1 M) in glass vial, which were slowly shaken by hand for several seconds, then placed at 80°C for 12 h. During the treatment, the CsCl solution (1 M) was refreshed twice. Then the crystals were taken out of solution and washed with deionized water to remove residual Cs^+ ions adsorbed on the crystal surface.

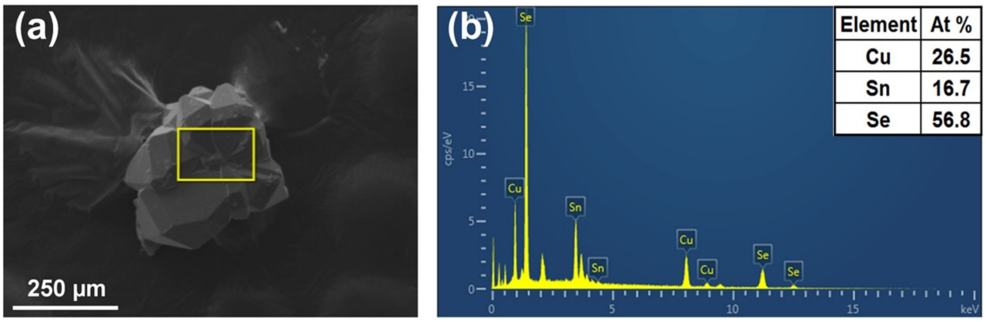

Fig. S1 (a) SEM images and (b) corresponding EDS of as-synthesized **COC-10-Se**.

(EDS elemental analysis of single crystal shows atomic ratio of Cu/Sn in COC-10-Se is 1.67, which is close to the calculated value 1.59).

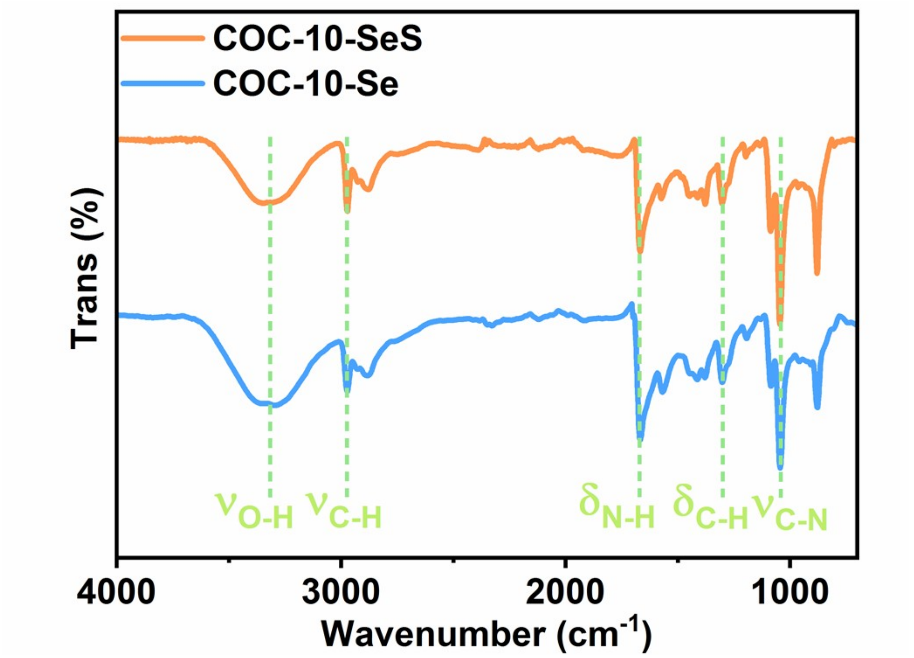

Fig. S2 FT-IR spectra of **COC-10-Se** and **COC-10-SeS**. The bands of IR at about 3235cm^{-1} belong to the stretching vibration of the O-H. The IR bands at 2972 cm^{-1}, 2874 cm^{-1} and 1301 cm^{-1} belong to the stretching vibration and bending vibration of the C-H of organic amines. The IR bands at 1658 cm^{-1} indicate the presence of N-H group. The broad vibration bands of IR at 1045 cm^{-1} belong to the stretching vibration of C-N.

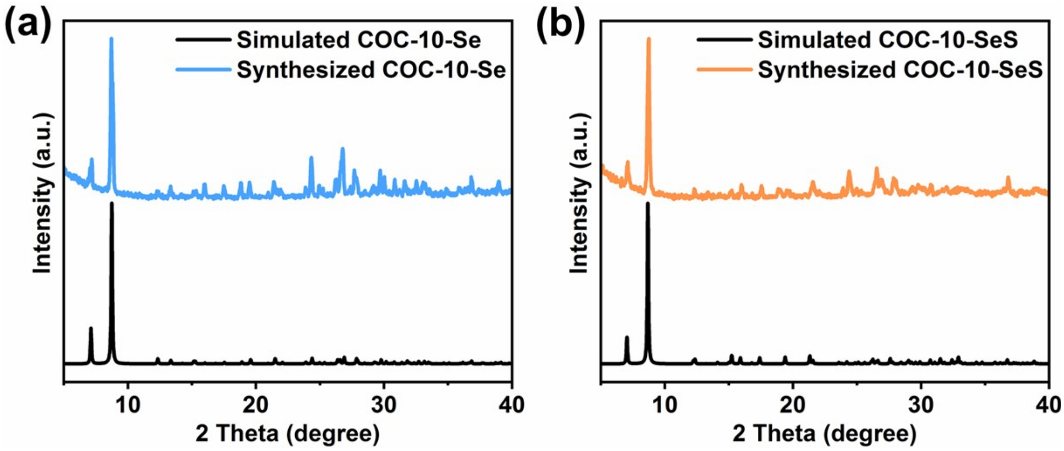

Fig. S3 The simulated and experimental PXRD patterns of (a) **COC-10-Se** and (b) **COC-10-SeS**.

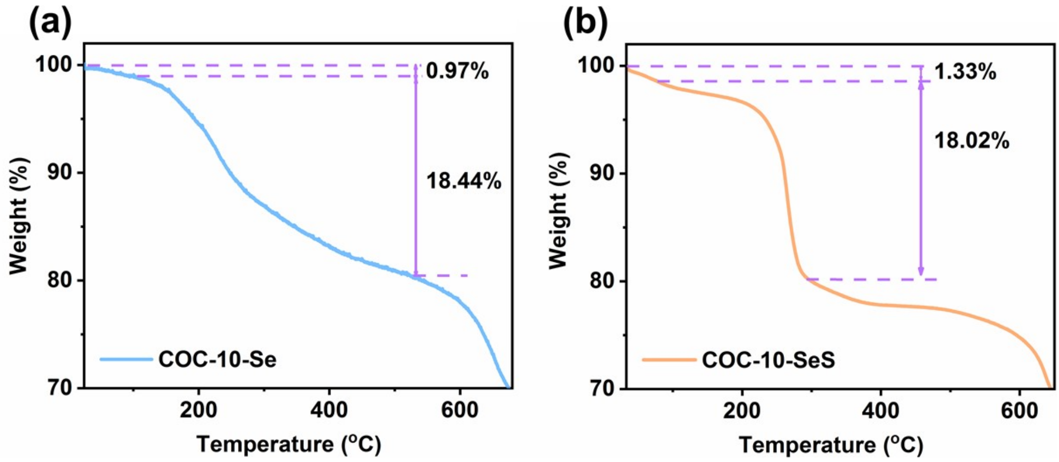

Fig. S4 Thermogravimetric (TG) analysis curves of (a) **COC-10-Se** and (b) **COC-10-SeS**. The first weight loss of 0.97 % and 1.33 % could be attributed to water molecules. The second weight loss of around 18.44% occurs between 100-525 ^{o}C and 18.02 % occurs between 100-300 ^{o}C, corresponding to the removal of charge-balanced organic amine molecules.

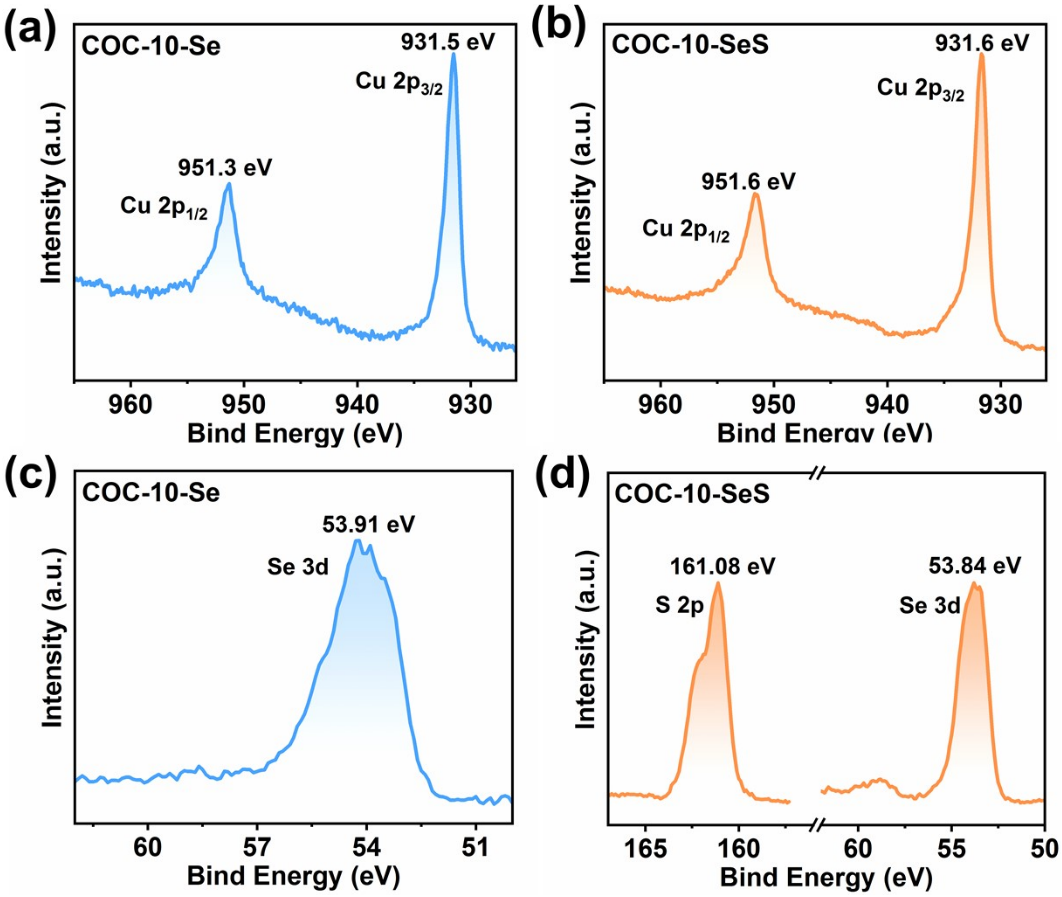

Fig. S5 High resolution XPS spectra of (a) Cu 2p and (c) Se 3d for **COC-10-Se;** (b) Cu 2p and (d) S 2p and Se 3d for **COC-10-SeS**.

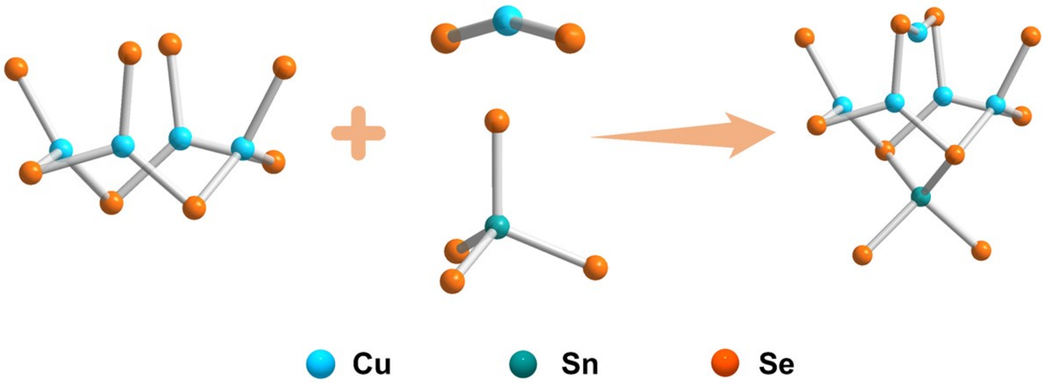

Fig. S6 Illustration of the assembly of [Cu_5SnSe_{10}] clusters.

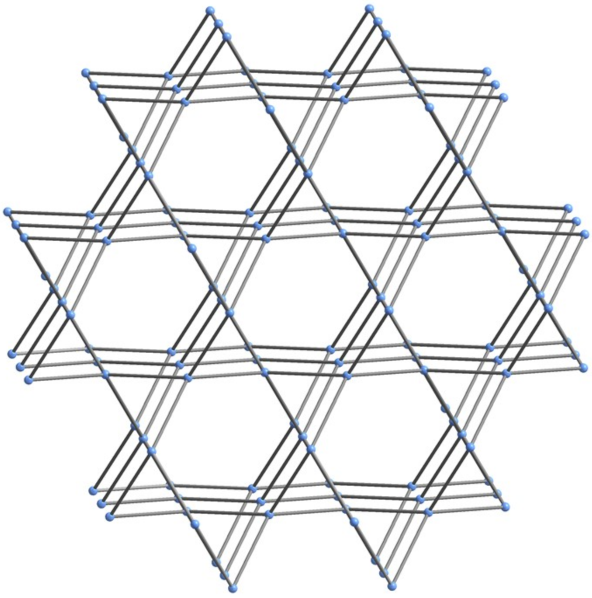

Fig. S7 The *qtz* topology of **COC-10-Se** viewed along *c* axis *via* treating [Cu_5SnSe_{10}] clusters as nodes (labeled as blue spheres) and $SnSe_4$ units as the linkers (labeled as grey bars).

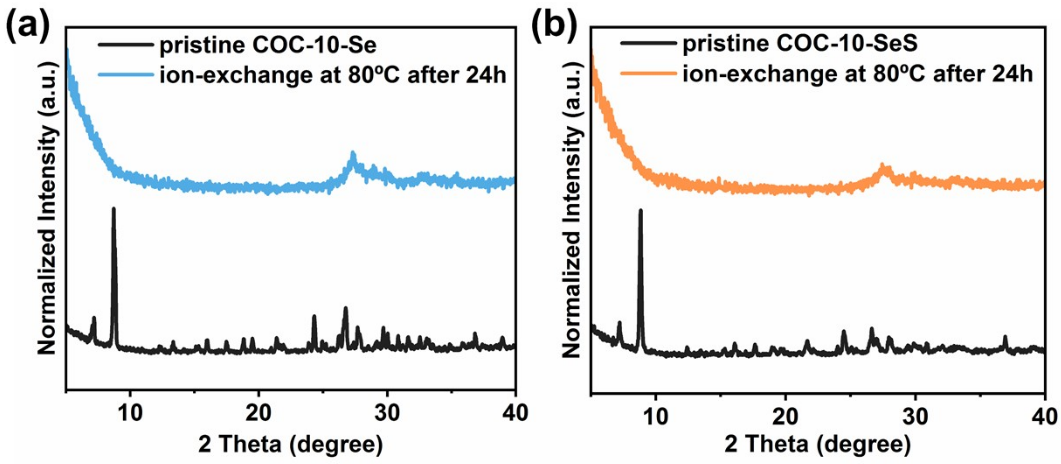

Fig.S8 The PXRD patterns of pristine and ion-exchanged (a) **COC-10-Se** and (b) **COC-10-SeS**.

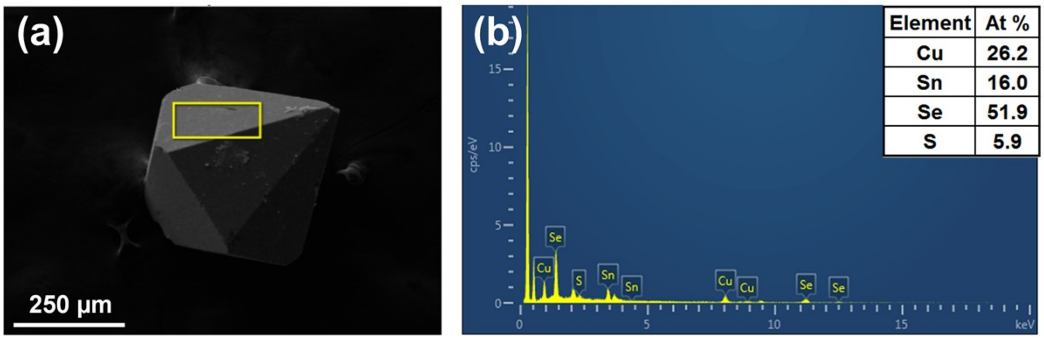

Element	At %
Cu	26.2
Sn	16.0
Se	51.9
S	5.9

Fig. S9 (a) SEM images and (b) corresponding EDS of as-synthesized **COC-10-SeS**. (EDS elemental analysis of single crystal shows atomic ratio of Cu/Sn in **COC-10-SeS** is 1.67, which is in good agreement with the calculated value 1.64. In addition, the atomic ratio of S/(Se + S) is about 0.102.)

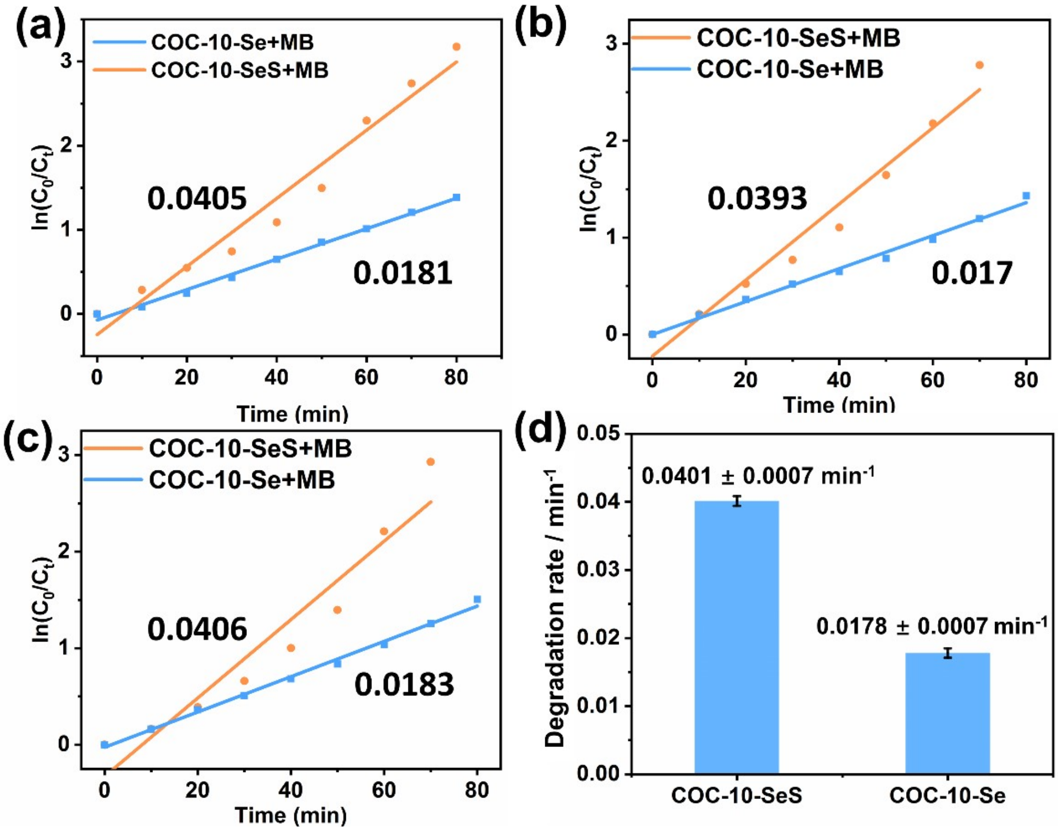

Fig. S10 (a-c) Calculated degradation rates of MB for **COC-10-Se** and **COC-SeS** in three parallel experiments; (d) Calculated average degradation rates of MB for **COC-10-Se** and **COC-SeS** with error bars.

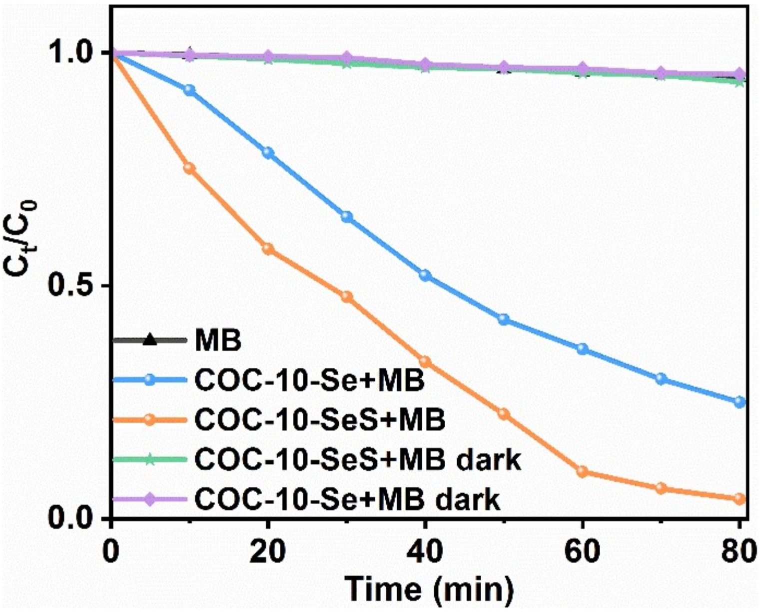

Fig. S11 Comparison of the photocatalytic degradation activities of **COC-10-Se** and **COC-10-SeS** under light irradiation and in the absence of light (dark experiments) as demonstrated by MB concentration versus irradiation time.

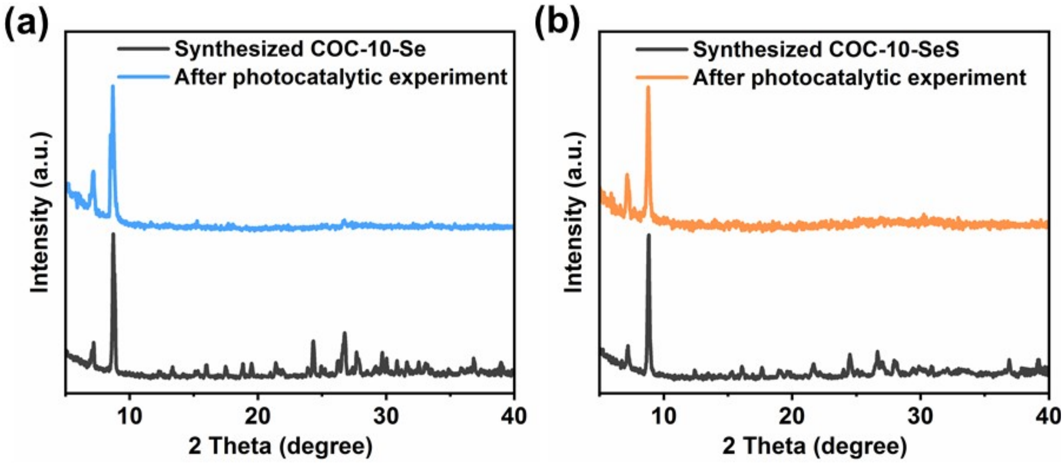

Fig. S12 PXRD patterns of **COC-10-Se** (a) and **COC-10-SeS** (b) before and after photocatalytic reactions.

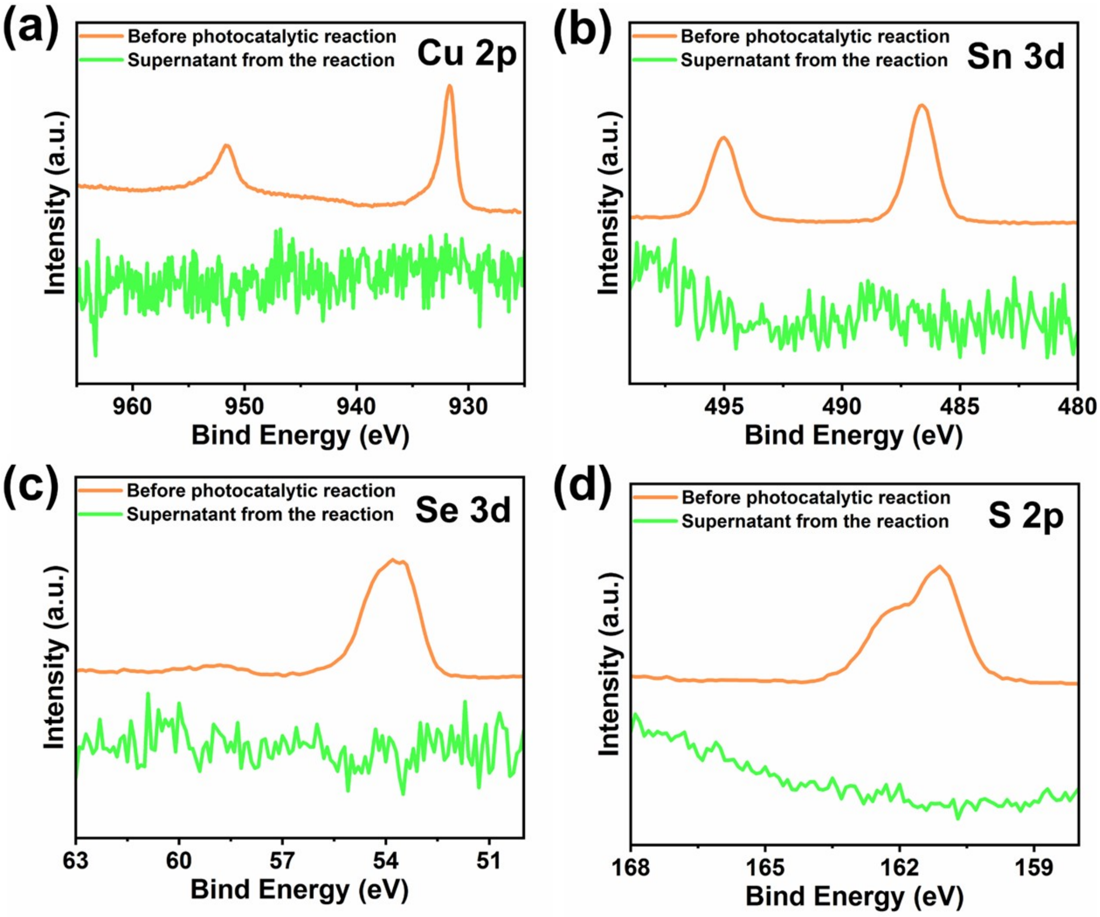

Fig. S13 Comparison of high resolution XPS spectra of (a) Cu 2p, (b) Sn 3d, (c) Se 3d and (d) S 2p for **COC-10-SeS** before photocatalytic reaction and the supernatant from the reaction.

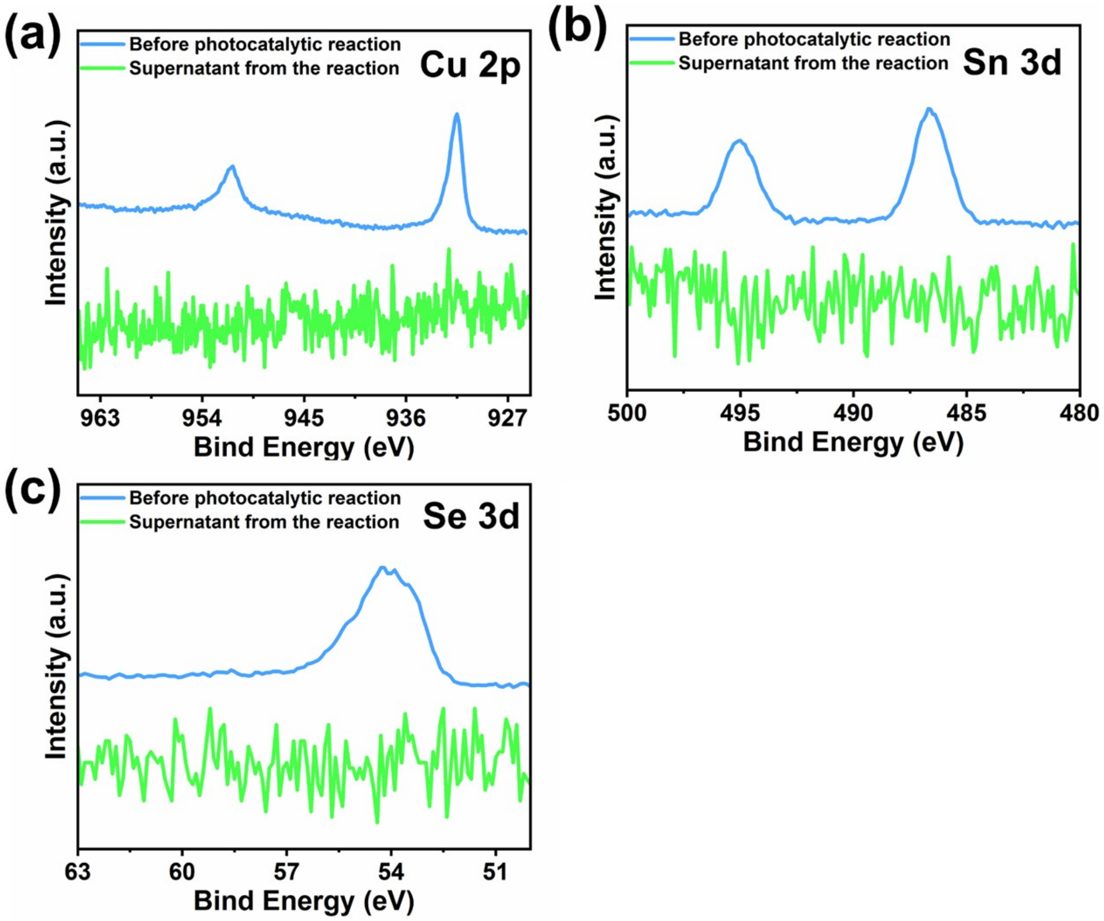

Fig.S14 Comparison of high resolution XPS spectra of (a) Cu 2p, (b) Sn 3d, (c) Se 3d for **COC-10-Se** before photocatalytic reaction and the supernatant from the reaction.

Table S1. Crystallographic data and structure refinement parameters for **COC-10-Se-*L***, **COC-10-Se-*D*** and **COC-10-SeS**.

Compounds	**COC-10-Se-*L***	**COC-10-Se-*D***	**COC-10-SeS**
Empirical formula	$Cu_{15}Se_{30}Sn_9C_{63}H_{123}N_{18}O_3$		$Cu_{15}S_3Se_{27}Sn_9C_{63}H_{123}N_{18}O_3$
Crystal system	hexagonal	hexagonal	hexagonal
Space group	$P6_4$	$P6_2$	$P6_2$
Z	1	1	1
a (Å)	14.4223(6)	14.2532(5)	14.4498(6)
b (Å)	14.4223(6)	14.2532(5)	14.4498(6)
c (Å)	17.4233(7)	17.4160(6)	17.4321(9)
α (deg.)	90	90	90
β (deg.)	90	90	90
γ (deg.)	120	120	120
V (Å^3)	3138.6(3)	3064.1(2)	3152.1(3)
Flack parameter	0.03(2)	0.04(2)	0.247(178
GOF on F^2	1.040	1.028	1.088
R_1, wR_2 ($I>2\sigma(I)$)	0.0330, 0.0694	0.0349, 0.0834	0.0344,0.0655
R_1, wR_2 (all data)	0.0631, 0.0818	0.0586, 0.0924	0.0480,0.0686

Table S2. Summary of copper-rich open-framework chalcogenides with different topologies.

Compound	**SBUs**	**Linker**	**Topology**	**Ref**
CuSnSe-1	Cu_8Se_{13} and Cu_4Se_{16}	$[SnSe_4]$	*pyr*	1
GeCuS-1	Cu_8S_{12}	$[Ge_2S_6]$ and $[GeS_4]$	*pcu*	2
1a	Cu_8Se_{13}	$[Ge_2Se_6]$	*pcu*	3
1b	Cu_8Se_{13}	$[Sn_2Se_6]$	*pcu*	3
1c	Cu_8S_{12}	$[Ge_2S_6]$	*pcu*	3
2	Cu_7GeSe_{13}	$[GeSe_4]$	*pcu*	3
COC-8	$[Cu_5(Sn_xM_{1-x})Se_{10}]^a$	$[(Sn_xM_{1-x})_2Se_6]^a$	*CrB_4*	4
COC-10-Se	$[Cu_5SnSe_{10}]$	$[SnSe_4]$	*qtz*	**This work**

^{a}M=In^{3+} or Ga^{3+} ions

References

1. H. Yang, L. Wang, D. Hu, J. Lin, L. Luo, H. Wang, T. Wu, *Chem. Commun.*, 2016, 52, 4140-4143.
2. Z. Zhang, J. Zhang, T. Wu, X. Bu, P. Feng. *J. Am. Chem. Soc.*, 2008, 130, 15238-15239.
3. M. Luo, D. Hu, H. Yang, D. Li, T. Wu, *Inorg. Chem. Front.*, 2017, 4, 387-392.
4. B. Han, J. Wang, Y. Liu, X. Wang, C. Xue, J. Lv, Z. Wu, R. Zhou, D. Xu, D.-S. Li, T. Wu, *Inorg. Chem.*, 2020, 59, 7919-7923.